WILEY-VCH

DOI: 10.1002/ ((please add manuscript number))
Article type: Full Paper

A Substitution-dependant Light-up fluorescence probe for selectively detecting Fe^{3+} ions and its cell imaging application

*Xing Feng, Ying Li, Xuewen He, Haixiang Liu, Zheng Zhao, Ryan T. K. Kwok, Mark R. J. Elsegood, Jacky W. Y. Lam, Ben Zhong Tang**

((Optional Dedication))

Dr. X. Feng, Dr. Y. Li, Mr. X. He, Mr. H. Liu, Dr. Z. Zhao, Dr. R. T. K. Kwok, Dr. J. W. Y. Lam, Prof. B. Z. Tang
Division of Biomedical Engineering, Department of Chemistry, Hong Kong Branch of Chinese National Engineering Research Center for Tissue Restoration and Reconstruction, Institute for Advanced Study, Institute of Molecular Functional Materials, State Key Laboratory of Molecular Neuroscience, The Hong Kong University of Science and Technology (HKUST), Clear Water Bay, Kowloon, Hong Kong, China.
E-mail: tangbenz@ust.hk.
Dr. X. Feng
School of Materials and Energy, Guangdong University of Technology, Guangzhou 510006, P. R. China.
Dr. M. R. J. Elsegood
Chemistry Department, Loughborough University, Loughborough, LE11 3TU, UK
Prof. B. Z. Tang
NSFC Center for Luminescence from Molecular Aggregates, SCUT-HKUST Joint Research Laboratory, State Key Laboratory of Luminescent Materials and Devices, South China University of Technology, Guangzhou 510640, P.R. China.
Prof. B. Z. Tang
HKUST-Shenzhen Research Institute, No. 9 Yuexing 1st RD, South Area, Hi-tech Park, Nanshan, Shenzhen 518057, P.R. China.

Keywords: aggregation-induced emission, molecular recognition, iron (III), acid dissociation constant, cell imaging

Delibrate design of specific and sensitive molecular probes with distinctive physicial/chemical properties for analytes sensing is of great significance. Herein, by taking advantage of the position-dependent substituent effects, an aggregation induced emission (AIE) featured iron (III) probe from *ortho*-substituted pyridinyl-functionalized tetraphenylethylene (TPE-*o*-Py) was synthesized. It displayed high sensitivity and selectivity toward Iron (III) detection. The recognition arises from the position isomer of *ortho*-substitution, and the fact that TPE-*o*-Py has a low acid dissociation constant (pKa) that is close to that of hydrolyzed Fe^{3+}. Importantly, TPE-*o*-Py as a light-up fluorescence probe

could be employed for iron (III) sensing in living cells with a pronounced red-shift in fluorescence color.

1. Introduction

Molecular recognition has attracted increasing attention because of its significant application in supramolecular chemistry and biological systems.[1] The association of two molecules interacting by self-assembly or self-organization processes, can exhibit distinctive photophysical properties, biological activities, as well as visible molecular dynamics.[2] However, optimizing molecular structure with appropriate affinity to achieve equilibration between sensitivity and selectivity for molecular recognition is still a great challenge.

Iron is an abundant and inexpensive metal, which has been widely used in the field of synthetic chemistry.[3] It also plays an indispensable role for living organisms, such as haematopoiesis, enzyme production, metabolic energy conversion and immune function maintenance.[4a] An abnormal concentration of iron in living systems would harm their normal physiological function.[4] Therefore, it is necessary to develop an efficient approach to monitor Fe^{3+} both in *vivo* and in *vitro*.[4b,5] Comparing with the traditional strategies based on absorption colorimetry or electrochemical techniques,[6] fluorescent Fe^{3+} probes showed advantages in higher sensitivity, faster responsiveness as well as greater practicability. In particular, a light-up type fluorescent probe offers a superiority in signal to noise ratio in target analyte recognition. Voelcker *et al.*, presented a light-up fluorescent sensor based on graphene quantum dots for Fe^{3+} imaging in cancer stem cells, which showed high sensitivity with a detection limit of 0.02 μM. The proposed mechanism of this fluorescent sensor depended on the switching of the spirolactam ring of rhodamine between on and off states in the presence and absence of Fe^{3+}, respectively.[7] However, the design of reversible molecular conformation for the specific recognition of Iron (III) is still rare.

On the other hand, the aggregation-induced emission (AIE) luminogens show unique turn-on fluorescence characteristics. They exhibit non-emissive behaviour when dissolved in

good solvents but emit strong fluorescence in poor solvents by forming aggregates.[8] The AIE phenomenon originates from the restriction of intramolecular rotations (RIR).[9] The unique light-up AIE properties have been widely applied in subcellular/cellular imaging, long-lasting tracking of bioactivity, and imaging guided therapy.[10] Our group previously demonstrated a 4-position pyridinyl-functionalized tetraphenylethylene AIEgen as a turn-on fluorescent probe for detection of trivalent cations, but it showed similar fluorescence responsiveness toward Cr^{3+}, Fe^{3+}, and Al^{3+} without obvious selectivity.[11] In fact, although many AIE-active fluorescent probes had been reported for various cations/anions with special characteristics, there was little research focus on light-up type AIE probes for specific Fe^{3+} detection in live cells.

Depending on the substitution effect for electronic density contribution, we designed and synthesized an *ortho*-substituted pyridinyl-functionalized tetraphenylethylene molecule (TPE-*o*-Py), which possessed pronounced AIE characteristics with high sensitivity and selectivity in Iron (III) detection in a THF/water mixture. More interestingly, when the TPE-*o*-Py meets Fe^{3+} in living cells, the strong orange-red fluorescence could be observed though a fluorescence microscope, indicating a potential application for iron monitoring in living systems.

2. Results and discussion

2.1. Synthesis

The compound TPE-*o*-Py was synthesized by the Mizoroki-Heck coupling reaction as shown in Scheme 1. The target chemical structure was confirmed by $^{1}H/^{13}C$ NMR spectra, single crystal X-ray diffraction and high-resolution mass spectrometry, as well as elemental analysis.

Insert Scheme 1 in here

2.2. Crystal structure

The single crystal of TPE-*o*-Py was grown by slow evaporation of a solution in a mixture of CH_2Cl_2 and hexane (1:1, vol/vol). Single crystal X-ray diffraction analysis at 150K revealed that TPE-*o*-Py crystallized in the monoclinic crystal system in space group *I*2/*a*. There are two molecules in the asymmetric unit (Figure 1). In the packing of the crystal structure, C−H···π intermolecular interactions dominate the contacts between neighbouring molecules. For example, the phenyl rings between neighboring molecules were associated together *via* several weak C–H···π interactions along the *c* axis.

Insert Figure 1 in here

Generally, in TPE-based molecules, the four phenyl rings can rotate freely in solution or in the gas phase. This motion serves as a channel for the excited state to decay non-radiatively. However, in this case, due to the restricted rotation of the four peripheral phenyl moieties by C−H···π interactions between neighbouring molecules in the crystalline state, the C=C bond of TPE can only undergo in-plane reorientations, named pedal motion.[13] This inhibited rotation of the phenyl groups may have contributed to the static disorder observed in the structure. Both alkene groups are two-fold disordered in the first molecule, and the occupancy ratio of C(1)/C(2):C(1X)/C(2X) is 0.54:0.46(2); the occupancy ratio of C(9)/C(10):C(9X)/C(10X) is 0.719:0.218(16). Similarly, both alkene groups are two-fold disordered in the second molecule, and the occupancy ratio of C(34)/C(35):C(34X)/C(35X) is 0.65:0.35(2); the occupancy ratio of C(42)/C(43):C(42X)/C(43X) is 0.637:0.036(16). In this system, the single-crystal X-ray diffraction analysis offered a visible manifestation of the consequences of a restriction of intramolecular motion (RIM) dependent AIE mechanism[9] at molecular level. One might imagine the molecules being unable to rotate freely during crystal growth and hence ending up disordered.

2.3. Photophysical properties

TPE-*o*-Py showed good solubility in various organic solvents, such as CH_2Cl_2, $CHCl_3$, THF, and toluene, but aggregated in poor solvents (i.e. deionized water). Herein, the UV-vis

spectrum of TPE-*o*-Py was examined in tetrahydrofuran (THF) solution, and is shown in Figure S6. The compound exhibited a low energy absorption band at 348 nm with a molar absorption coefficient of 63734 cm^{-1} M^{-1}, corresponding to the absorption of π–π* transitions of the conjugated π-electron system in the TPE unit. Previous work indicated the position of the pyridyl nitrogen atom has a strong effect on the photophysical properties both in solution and the solid state.[14] However, the location of the N atom at the 2-position or 4-position in TPE-Py system gives similar optical characteristics, so shows a limited effect on electron transitions.[14b]

Insert Figure 2 in here

To investigate the AIE characteristics in detail, different volume fractions of water (f_w) were added to the pure THF solutions of TPE-*o*-Py (10 μM). Obviously, when f_w < 70%, TPE-*o*-Py emitted relatively weak FL signals with the maximum peak located at 472 nm. However, after increasing above this point, the emission intensity enhanced dramatically, with about 10-fold enhancement at f_w = 90% compared with that in pure THF solution (Figure 2b), indicating its pronounced AIE property.[9] Even in the solid state, this TPE-*o*-Py displayed strong sky-blue emission with a maximum at 486 nm. The fluorescence quantum yields dramatically increased from 0.06 (in THF solution) to 0.58 (in the solid state).

Insert Figure 3 in here

The pyridine moiety is an excellent ligand which prefers to coordinate with transition and lanthanide metals in the periodic table;[15] also, pyridine-containing fluorescent probes show considerable affiliation to metal cations both in *vitro* and *vivo*.[16] Due to the N atom of pyridine being in the 2-position instead of the 4-position, the compound tended to form complexes more easily with lanthanide metals, by coordinating via the N atom and olefin moieties.[17] However, after adding an amount of Ir^{3+} and Ru^{3+} to a mixture of THF-H_2O (f_w = 70%) solution containing TPE-*o*-Py (10 mM), no obvious fluorescence changes were observed. As with our previous application of isomer TPE-*p*-Py as a colorimetric and

ratiometric fluorescent probe to Fe^{3+}, Al^{3+} and Cr^{3+},[11] herein ,we attempt to use TPE-*o*-Py as a "turn-on" fluorescence probe to detect trivalent cations (Fe^{3+}, Al^{3+}, and Cr^{3+}). As Figure 3 shows, there were no obvious changes in the fluorescence spectra of TPE-*o*-Py after mixing with various cations (such as Na^{+}, K^{+}, Ca^{2+}, Mg^{2+}, Al^{3+}, Cd^{2+}, Co^{2+}, Cr^{2+}, Cu^{2+}, Fe^{2+}, Hg^{2+}, Mn^{2+}, Ni^{2+}, Sr^{2+}, Zn^{2+}, Al^{3+}, and Cr^{3+}, etc.) even at concentrations up to 10^{-5} M. Notably, only the response to Fe^{3+} was highly selective. It is noticeable that the fluorescence spectra of TPE-*o*-Py showed a gradual red-shift from 450 nm to 578 nm with increasing concentrations of Fe^{3+}. These interesting results inspired us to deeply explore the inherent relationship between molecular conformation and coordination ability to the Fe^{3+} ion.

According to our report,[11] the M^{3+} (Fe^{3+}, Al^{3+}, and Cr^{3+}) was intensively hydrolyzed in water which leads to a protonated TPE-*p*-Py, which exhibits a red emission by an intramolecular charge transfer (ICT) effect. To prove this concept, the stability of TPE-*o*-Py in THF solution and at different pH values was investigated by UV-vis and PL spectra. As shown in Figure 4, the maximum absorption of TPE-*o*-Py was at 348 nm in pure THF. Also, the absorption profile presented slightly changes at different pH values (from 3.0 to 10.0). However, when pH < 3.0, the absorption spectra displayed a slight red-shift with decreased intensity. The absorption maximum was further shifted to 372 nm when pH = 2.0, indicating the TPE-*o*-Py could be protonated in the presence of strong acidic solution and leads to the intramolecular charge transfer (ICT) effect. More detailed information was observed in the PL spectrum. The PL spectrum of TPE-*o*-Py exhibits a broad peak at 472 nm when the pH value was higher than 3.0, and no change was observed except the emission intensity slightly decreased. However, when the pH < 3.0, a new peak appeared at 573 nm with the broad spectrum covering the whole visible range (400-650 nm). With the pH value progressivly decreasing to 1.0, the emission peak was further shifted to 595 nm with an increased emission intensity. Indeed, the pH value played a significant role in the absorption and emission profile of the TPE-*o*-Py molecule.

Insert Figure 4 in here

Further, we carefully examined the position isomer effect of the N atom for the acid dissociation constant (pK_a) of TPE-*o*-Py.[18] According to our calculations from emission intensity ratios *versus* pH value, the pK_a value is 3.27 for TPE-*o*-Py.[19] This suggested that the PL spectra would be changed greatly when the pH was lower than 3.27. Figure S7 illustrates the fluorescence titration experiments of TPE-*o*-Py with the Fe^{3+} in a mixture of THF-H_2O (f_w = 70%) solution. Upon addition of Fe^{3+} to 2.0×10^{-5} M, a remarkable red-shift of the emission maximum from 472 nm to 564 nm was observed. In addition, as the concentration of Fe^{3+} was increased, the PL intensity red fluorescence centered at 564 nm decreased with a slight red-shift from 564 to 573 nm due to the enhanced TICT effect. The PL spectra feature exhibited a slight red-shift before and after the addition of Al^{3+} (Figure 4c and Figure S8). In addition, the fluorescene probe can recognize Fe^{3+} with a considerable detection limit (1.04×10^{-5} M). The pK_a values of the metal ions were calculated and summarized in Table 1. Only the pKa (2.56) of Fe^{3+} was lower than that of TPE-o-Py (3.27). This is due to the hydrolyzation of Fe^{3+} in water and the ionized hydrogen protons that result from decreasing the pH of solution to lower than 3.27. On the other hand, owing to the nature of the different solubility products (Ksp) of the metal ions, it was difficult to decrease the pH to 3.27 and protonate TPE-*o*-Py in aqueous solution in the presence of Al^{3+} or Cr^{3+}. In addition, because of the pK_a of 5.62 and 4.98 for 4-Vinylpyridine and 2-Vinylpyridine, respectively,[18] we could also infer that the pKa of TPE-*p*-Py was higher than that of TPE-*o*-Py, making it easy to protonate in hydrolyzing M^{3+} (Fe^{3+}, Al^{3+}, and Cr^{3+}) solution.

To explore the proton effect for the electronic coupling of the TPE-*o*-Py molecule, the optimized molecular geometries in the ground-state of TPE-*o*-Py and H^+@TPE-*o*-Py were calculated by Gaussian 09W using the B3LYP/6-31G* basis set.[20] In TPE-*o*-Py and H^+@TPE-*o*-Py, the olefin bridge caused planarization of the π-system (torsion angle <2.1°) between the pyridine ring within the TPE fragment. As a result, the HOMO of TPE-*o*-Py is

primarily located on the donor (i.e. pyridine moiety), and the LUMO is mostly delocalized on the TPE and partially on the extended π-conjugation. Whereas, in H^+@TPE-*o*-Py, the HOMO is mainly spread over the whole molecule and the LUMO localized on the protonated pyridine moieties and C=C bond. This result indicates that the H^+@TPE-*o*-Py underwent an ICT transition through an extending π-conjugation. Indeed, the HOMO−LUMO gap value of H^+@TPE-*o*-Py (E_g = 1.69 eV) was lower than that of TPE-o-Py (E_g = 3.43 eV), leading to the red shift in absorption and emission spectra, which is in accord with our observations in the above experiments.

2.4. Cell imaging

Depending on the pH value effect, the high sensitivity and selectivity TPE-*o*-Py for detecting Fe^{3+} was then explored in *vitro* cellular imaging by confocal fluorescence microscopy. The HeLa and MCF-7 (breast cancer) cells were incubated with and without Fe^{3+} in medium for 2 h at 37 ^oC, and then washed three times with PBS buffer (pH = 7.4) to eliminate extra Fe^{3+}. The treated living cells were re-incubated with TPE-*o*-Py (10 μM) for 0.5 h, before directly imaging under a confocal fluorescence microscope without further washing. In Figure 5 and Figure S10, the confocal section images of HeLa and MCF-7 cells exhibit normal morphology with good health. In the absence of Fe^{3+}, the HeLa cells emitted deep blue fluorescence after being incubated with TPE-*o*-Py, while in the presence of Fe^{3+}, blue and red fluorescence appeared simultaneously. As the concentration of Fe^{3+} was increased, the intensity of red fluorescence also enhanced, in agreement with the observation in THF/water. Further, the TPE-*o*-Py showed excellent biological compatibility even at 80 μm concentration (Figure 6). The results revealed that TPE-*o*-Py could be potentially utilized as a biolabel to respond to Fe^{3+} both in HeLa and MCF-7 cells.

Insert Figure 5 in here

In addition, the cytotoxicity of TPE-*o*-Py was further evaluated using Calcein acetoxymethyl ester (AM)/propidium iodide (PI) assay (live/dead) kit and CCK8 assay. As

shown in Figure 6, The HeLa cells and MCF-7 cells exhibited green fluorescence at various concentrations of TPE-*o*-Py ranging from 0 to 80 μM. The cells distributed in radial or swirl patterns covering the plate surface and displayed normal cell morphology with spindle shapes, without dead cells appearing. The cell viability results showed that the viability of both cells remains close to 100% (> 95%) over 24 h at a concentration of 80 μM, indicating the low cytotoxicity of TPE-*o*-Py.

Insert Figure 6 in here

3. Conclusions

A novel, ortho-substituted, pyridinyl-functionalized tetraphenylethylene TPE-*o*-Py was successfully synthesized via the Mizoroki-Heck coupling reaction. The AIE-active TPE-*o*-Py molecule exhibited weak emission in solution but strong fluorescence intensity in the aggregated state. Among various metal ions, only Fe^{3+} can induce the alteration in the fluorescence emission feature of TPE-*o*-Py from weak blue to strong red color. Furthermore, only the hydrolyzed Fe^{3+} can induce the protonation of TPE-o-Py, because of its lower acid dissociation constant (pKa) which was close to that of hydrolyzed Fe^{3+}. This is the first example of a TPE derived fluorescence probe possessing characteristics including pH-dependence, turn-on capability, and ratiometric fluorescence for Fe^{3+} detection in live cells. The novel AIE-active TPE-*o*-Py is expected to be promising in the application of biological imaging and biomedical research in the future.

4. Experimental Section

*General***:** $^{1}H/^{13}C$ NMR spectra (400 MHz) were recorded on a Mercury plus 400MHz NMR spectrometer respectively, and referenced to 7.26 and 77.0 ppm for chloroform-D solvent with $SiMe_4$ as an internal reference: *J*-values are given in Hz. High-resolution mass spectra (HRMS) were taken on a GCT premier CAB048 mass spectrometer operating in a MALDI-TOF mode. Elemental analysis was performed on a ThermoFinnigan Flash EA1112

apparatus. FL spectra were recorded on a Hitachi 4500 spectrofluorometer. UV-vis absorption spectra were obtained on a Milton Ray Spectrofluorometer. Fluorescence quantum yields were measured using absolute methods. The quantum chemistry calculation was performed on the Gaussian 09W (B3LYP/6–31G* basis set) software package.

Crystallography: Crystallographic data for TPE-*o*-Py were collected on a Bruker APEX 2 CCD diffractometer with graphite-monochromated Mo Kα radiation (λ = 0.71073 Å) in the ω-scan mode. Crystal data. $C_{33}H_{25}N$, M = 435.54, monoclinic, a = 36.579(7), b= 5.6069(11), c = 47.597(13) Å, β = 100.227(3)°, U = 9607(4) Å^3, T = 150(2) K, space group $I2/a$, Z = 16, 1.7 ≤ θ ≤ 22.5°, 38508 reflections measured, 6237 unique (R_{int} = 0.067), which were used in all calculations. The final R = 0.089 (4561 observed data with $F^2 > 2\sigma(F^2)$, w$R(F^2)$ = 0.212 (all data) for 690 parameters, S = 1.04. Largest difference electron density features within ±0.64 e Å^{-3}. H atoms were constrained in a riding model. There are two molecules in the asymmetric unit. Both alkene groups were modelled as two-fold disordered in both molecules with restraints on anisotropic displacement parameters. The major component occupation factors at the following sites were as follows: at C(1)/C(2) = 54(2)%; at C(9)/C(10) = 71.9(16)%; at C(34)/C(35) = 65(2)%; at C(42)/C(43) = 63.7(16)%. The disorder arises because the space occupied by these or adjacent groups is similar in two different orientations. CCDC 1836698 contains the supplementary crystallographic data for this paper. These data can be obtained free of charge from The Cambridge Crystallographic Data Centre via www.ccdc.cam.ac.uk/data_request/cif.

Materials: Unless otherwise stated, all reagents used were purchased from J&K Chemicals or Sigma-Aldrich and were used without further purification. The solvent tetrahydrofuran (THF) was distilled prior to use. The 1-(4-Bromophenyl)-1,2,2-triphenylethylene was prepared as described previously.[12] The stock solutions of metal ions were prepared from $CdCl_2 \cdot 2.5H_2O$, $CoCl_2 \cdot 6H_2O$, $CuSO_4$, $FeCl_3$, $HgCl_2$, LiCl, $MgCl_2 \cdot 6H_2O$, $NiCl_2 \cdot 6H_2O$, $Pb(NO_3)_2$, $Zn(NO_3)_2 \cdot 7H_2O$, $AgNO_3$, $AlCl_3$, $CrCl_3$, $IrCl_3 \cdot xH_2O$, KCl, NaCl and NH_4Cl with doubly

distilled water. Dulbecco modified eagle medium (DMEM), fetal bovine serum (FBS), penicillin G (100 U mL^{-1}), streptomycin (100 U mL^{-1}), and 0.25% trypsin-0.53 mM EDTA solution were from Gibco (USA). HeLa cells and MCF-7 cells were from the Cell Bank of Peking Union Medical College (China). Calcein AM/ PI was from Dojindo (Japan).

Synthesis of compound (E)-2-(4-(1,2,2-triphenylvinyl)styryl) pyridine (TPE-o-Py): Into a 50 mL, two necked, round-bottom flask were added (2-(4-bromophenyl)ethene-1,1,2-triyl)tribenzene (495 mg, 1.2 mmol, 1.0 eq), potassium phosphate (429 mg, 2 mmol, 2 eq), palladium(II) acetate (14 mg, 0.06 mmol, 0.05 eq). The flask was filled with nitrogen. Dimethylacetamide (3 mL) and 2-vinylpyridine (0.2 mL, 1.8 mmol, 1.5 eq) were injected to the flask. The mixture was warmed to 145 ^{o}C for 72 h. After cooling to room temperature, the mixture was poured into 50 mL water and extracted with DCM (50 mL × 2). The collected organic layer was filtered and washed with brine twice, then dried over anhydrous magnesium sulfate. After solvent evaporation, the crude product was purified by silica-gel column chromatography using DCM/methanol (15:1 by volume) as eluent. A yellow solid of *(E)-2-(4-(1,2,2-triphenylvinyl)styryl)pyridine (TPE-o-Py)* was obtained. (320 mg, 61%). ^{1}H NMR (400 MHz, $CDCl_3$): δ_H = 7.01-7.12 (m, 19H), 7.30-7.34 (m, 3H), 7.52 (d, *J* = 16.0 Hz, 1H), 7.63 (t, 1H), 8.57 (d, *J* = 4.0 Hz, 1H) ppm; ^{13}C NMR (100 MHz, $CDCl_3$): δ_C = 155.07, 149.03, 143.36, 143.05, 143.01, 142.94, 140.69, 139.90, 135.86, 134.02, 131.82, 131.11, 130.78, 130.72, 127.15, 127.09, 127.01, 125.95, 125.90, 125.83, 121.33, 121.30 ppm; HRMS (MALDI−TOF) (ESI): m/z $[M + H]^+$ calcd for $C_{33}H_{25}N$ 435.1987 $[M^+]$; found 436.2.

Cell fluorescence: HeLa cells and MCF-7 cells were incubated in DMEM medium supplemented with 10% FBS at 37°C in a humidified atmosphere of 5% CO_2, which were seeded in confocal dishes (10^5 cells/well) in 2 mL culture medium. After incubation 24 h, the cells were treated with Fe^{3+} solutions (0 μM, 25 μM and 50 μM) for 2h and washed 3 times with PBS buffer (pH = 7.4) to remove any excess Fe^{3+}. The treated HeLa cells and MCF-7

cells were then incubated with TPE-*o*-Py (10 μM) in medium for 0.5 h. Then the HeLa cells and MCF-7 cells were washed with PBS buffer 3 times, the cells were imaged by a confocal laser scanning microscope (CLSM) (LSM710, Carl Zeiss, Germany).

Cytotoxicity Assay of TPE-o-Py: Calcein AM/PI kit : Calcein AM/PI kit was used to analyze the cell viability and morphology of HeLa cells and MCF-7 cells cultured in medium (DMEM + 10% FBS + 1% PS) with different concentrations of TPE-o-Py (0, 5, 10, 20, 40, 80 μM). The cells (1×10^5 cells mL^{-1}) were seeded in confocal dishes and incubated for 24 h (37 °C, 5% CO_2 humidified atmosphere). The medium was removed, and then different concentrations of TPE-o-Py were added and the cells were incubated for another 24 h. The culture medium was removed from the dishes and the cells were washed with PBS twice, 500 μL calcein AM/PI mixed solution was added into each well and the mixture was incubated for 20 min. Calcein AM/PI mixture was removed from the dish, the cells were washed with PBS once and 200 μL PBS was added before observing by a CLSM.

CCK8 assay: HeLa cells and MCF-7 cells were cultured on 96-well plates (1×10^4 cells 200 mL^{-1}) for 24 h. The culture medium was removed and 200 μL medium containing different concentrations of TPE-o-Py (0, 5, 10, 20, 40, 80 μM) was added and incubated for 24 h. The culture medium was removed and 100 μL CCK8 medium (90 μL medium and 10 μL CCK8 solution) (Dojindo, Japan) was added into each well and the samples were incubated for 1 h, then optical density (OD) of the samples was measured on a microplate reader (Tecan, infinite M200, Switzerland) at 450 nm. The results were analyzed by OriginPro 8.0.

Supporting Information

Supporting Information is available from the Wiley Online Library or from the author.

Acknowledgements

X. Feng and Y. Li contributed equally to this work. This work was supported by the National Science Foundation of China (21602014, 21788102 and 51620105009), the Research Grants Council of Hong Kong (16305015, N_HKUST604/14), the Innovation and

Technology Commission (ITC-CNERC14SC01), the Science and Technology Plan of Shenzhen (JCYJ20160229205601482 and JCY20170818113602462)

Received: ((will be filled in by the editorial staff))
Revised: ((will be filled in by the editorial staff))
Published online: ((will be filled in by the editorial staff))

References

[1] a) X.-L. Ni, X. Zeng, C. Redshaw, T. Yamato, *J. Org. Chem.* **2011**, *76*, 5696; b) S. J. Barrow, S. Kasera, M. J. Rowland, J. d. Barrio, O. A. Scherman, *Chem. Rev.* **2015**, *115*, 12320; c) G. Yu, K. Jie, F. Huang, *Chem. Rev.* **2015**, *115*, 7240; d) M. W. Peczuh, A. D. Hamilton, *Chem. Rev.* **2000**, *100*, 2479; e) K. Ariga, H. Ito, J. P. Hill, H. Tsukube, *Chem. Soc. Rev.* **2012**, *41*, 5800.

[2] a) J. M. Abendroth, O. S. Bushuyev, P. S. Weiss, C. J. Barrett, *ACS Nano* **2015**, *9*, 7746; b) J. F. Stoddart, *Acc. Chem. Res.* **2001**, *34*, 410; c) M. A. Watson, S. L. Cockroft, *Chem. Soc. Rev.* **2016**, *45*, 6118.

[3] C. Bolm, J. Legros, J. L. Paih, L. Zani, *Chem. Rev.* **2004**, *104*, 6217.

[4] a) N. Abbaspour, R. Hurrell, R. Kelishadi, *J Res Med Sci*. **2014**, *19*, 164; b) K. N. Raymond, E. A. Dertz, S. S. Kim, *Proc Natl Acad Sci USA.* **2003**, *100*, 3584; c) K. Pantopoulos, S. K. Porwal, A. Tartakoff, L. Devireddy, *Biochemistry* **2012**, *51*, 5705.

[5] a) N. Narayanaswamy, T. Govindaraju, *Sens. Actuators, B* **2012**, *161*, 304; b) J. Zou, X. Wang, L. Zhang, J. Wang, *Chem. Res. Toxicol.* **2015**, *28*, 373.

[6] L. R. Kindra, C. J. Eggers, A. T. Liu, K. Mendoza, J. Mendoza, A. R. K. Myers, R. M. Penner, *Anal. Chem.* **2015**, *87*, 11492.

[7] R. Guo, S. Zhou, Y. Li, X. Li, L. Fan, N. H. Voelcker, *ACS Appl. Mater. Interfaces* **2015**, *7*, 23958.

[8] a) J. Mei, N. L. C. Leung, R. T. K. Kwok, J. W. Y. Lam, B. Z. Tang, *Chem. Rev.* **2015**, *115*, 11718; b) X. Lou, Y. Zhuang, X. Zuo, Y. Jia, Y. Hong, X. Min, Z. Zhang, X. Xu, N. Liu, F. Xia, B. Z. Tang, *Anal. Chem.* **2015**, *87*, 6822.

[9] a) J. Luo, Z. Xie, J. W. Y. Lam, L. Cheng, H. Chen, C. Qiu, H. S. Kwok, X. Zhan, Y. Liu, D. Zhu, B. Z. Tang, *Chem. Commun.* **2001**, 1740; b) Y. Hong, J. W. Y. Lam, B. Z. Tang, *Chem. Soc. Rev.* **2011**, *40*, 5361; c) Y. Hong, J. W. Y. Lam, B. Z. Tang, *Chem. Commun.* **2009**, 4332.

[10]a) H. Shi, R. T. K. Kwok, J. Liu, B. Xing, B. Z. Tang, B. Liu, *J. Am. Chem. Soc.* **2012**, *134*, 17972; b) M. Gao, B. Z. Tang, *Drug Disscov. Today* **2017**, *22*, 1288; c) C. Gui, E. Zhao, R. T. K. Kwok, A. C. S. Leung, J. W. Y. Lam, M. Jiang, H. Deng, Y. Cai, W. Zhang, H. Su, B. Z. Tang, *Chem. Sci.* **2017**, *8*, 1822; d) Y. Yuan, B. Liu, *Chem. Sci.* **2017**, *8*, 2537; e) X. Gu, R. T. K. Kwok, J. W. Y. Lam, B. Z. Tang, *Biomaterials* **2017**, *146*, 115; f) Y. Cheng, J. Dai, C. Sun, R. Liu, T. Zhai, X. Lou, F. Xia, *Angew. Chem. Int. Ed.* **2018**, *57*, 3123.

[11]X. Chen, X. Yuan Shen, E. Guan, Y. Liu, A. Qin, J. Z. Sun, B. Z. Tang, *Chem. Commun.* **2013**, *49*, 1503.

[12]Z. Zhao, S. Chen, C. Y. K. Chan, J. W. Y. Lam, C. K.W. Jim, P. Lu, Z. Chang, H. S. Kwok, H. Qiu, B. Z. Tang, *Chem. Asian J.* **2012**, *7*, 484.

[13]a) J. Harada, K. Ogawa, *Chem. Soc. Rev.* **2009**, *38*, 2244; b) M. A. Kochman, A. Bil, C. A. Morrison, *Phys. Chem. Chem. Phys.* **2013**, *15*, 10803.

[14]a) R. Tang, X. Wang, W. Zhang, X. Zhuang, S. Bi, W. Zhang, F. Zhang, *J. Mater. Chem. C* **2016**, *4*, 7640; b) J. B. Pollock, T. R. Cook, G. L. Schneider, D. A. Lutterman, A. S. Davies, Peter J. Stang, *Inorg. Chem.* **2013**, *52*, 9254.

[15]a) J. M. Stauber, A. L. Wadler, C. E. Moore, A. L. Rheingold, J. S. Figueroa, *Inorg. Chem.* **2011**, *50*, 7309; b) C.-Y. Lin, J. C. Fettinger, P. P. Power, *Inorg. Chem.* **2017**, *56*,

9892–9902; c) S. Alvarez, *Chem. Rev.* **2015**, *115*, 13447; d) C.-G. Wang, Y.-H. Xing, Z.-P. Li, J. Li, X.-Q. Zeng, M.-F. Ge, S.-Y. Niu, *Cryst. Growth Des.* **2009**, *9*, 1525.

[16]a) S. Madhu, D. K. Sharma, S. K. Basu, S. Jadhav, A. Chowdhury, M. Ravikanth, *Inorg. Chem.* **2013**, *52*, 11136; b) N. Zhao, M. Li, Y. Yan, J. W. Y. Lam, Y. L. Zhang, Y. S. Zhao, K. S. Wong, B. Z. Tang, *J. Mater. Chem. C* **2013**, *1*, 4640; c) F. Miao, G. Song, Y. Sun, Y. Liu, F. Guo, W. Zhang, M. Tian, X. Yu, *Biosens. Bioelectron.* **2013**, *50*, 42.

[17]B. L. Small, *Acc. Chem. Res.* **2015**, *48*, 2599.

[18]a) R. J. Gillespie, E. A. Robinson, *J Comput. Chem.* **2006,** *28***,** 87; b) M. O'Neil, Ed., *The Merck Index, 14th Edition*, Merck & Co., Whitehouse Station, NJ, USA **2006**; c) I. M. Kolthoff, P. J. Elving, F. H. Stross, *Treatise on Analytical Chemistry, 2nd edition*, Wiley-Interscience, Verlag GmbH & Co. KGaA, Weinheim, **1993**.

[19]A. M. Brown, *Comput. Meth. Prog. Bio*. **2001**. *65*, 191.

[20]M. J. Frisch, GAUSSIAN 09, revision C.01; Gaussian Inc.: Wallingford, CT, **2009**.

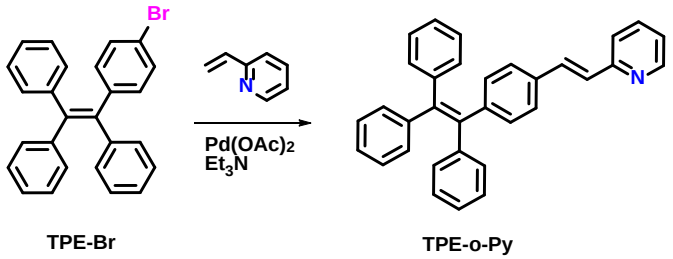

Scheme 1 the synthetic route to TPE-*o*-Py.

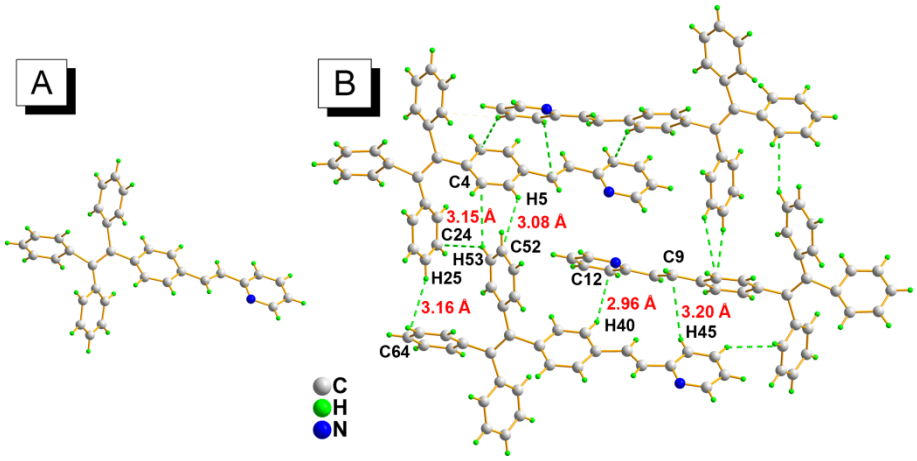

Figure 1 (left) Crystal structure of TPE-o-Py and (right) multiple C-H···π interactions between neighboring molecules. Minor disorder components have been omitted for clarity.

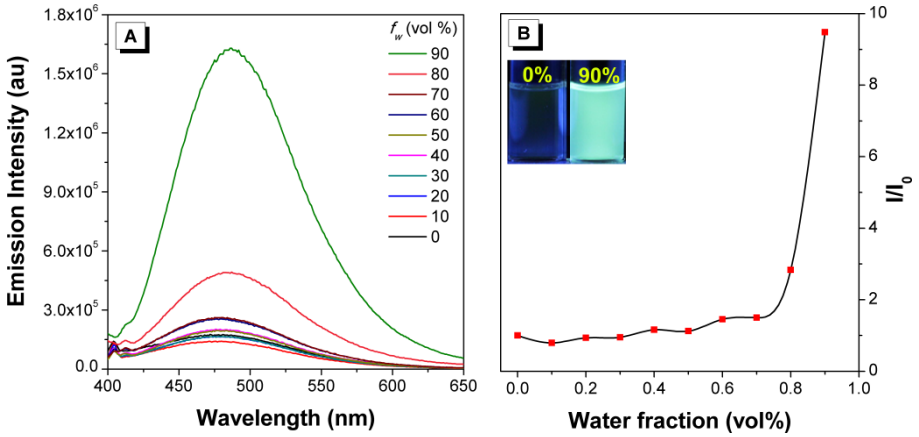

Figure 2 A) PL spectra of TPE-*o*-Py in THF/water mixtures with different water fractions. B) Plots of I/I_0 values versus the compositions of THF/water mixtures, in which I_0 is the PL intensity in pure THF solution. Inset: photographs in THF/water mixtures (f_w = 90%) taken under 365 nm UV irradiation.

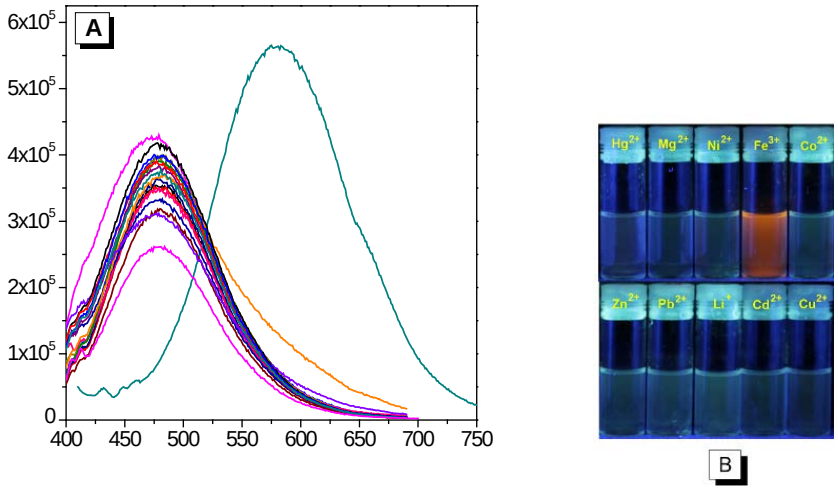

Figure 3. (A) PL spectra of TPE-p-Py in THF and in THF/water mixture in the presence of 700 μM of different metal cations. (B) Photographs of the above solutions taken under UV light (λex = 365 nm) and daylight, respectively. Concentration of [TPE-*o*-Py] = 10 μM.
[I don't understand the comment about the photographs, as I can only see one photograph of each solution, so how can there be both a photograph taken under UV light and one taken in daylight?]

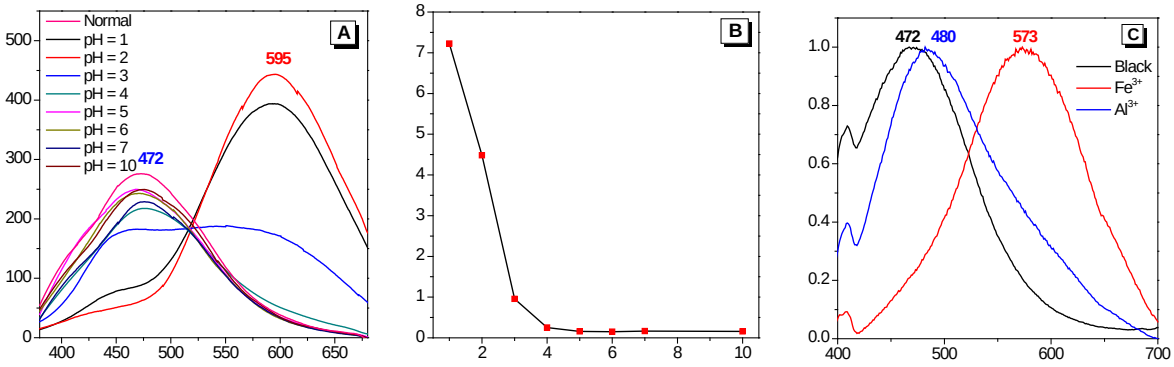

Figure 4. (A) PL spectra of TPE-*o*-Py (10 μM) in different pH value buffers. (B) Plot of I_{595}/I_{472} (ratio of intensity at 595 nm to intensity at 472 nm) versus pH value, insert: photographs in different pH value (pH = 1 and pH = 14) taken under 365 nm UV irradiation. (C) Normalization of PL spectra of TPE-*o*-Py (10 μM) upon addition of Fe^{3+} and Al^{3+} (100 μM) in THF/H_2O (f_w = 70%) at 298 K (λex = 350 nm). [There are no inserted photographs for B]

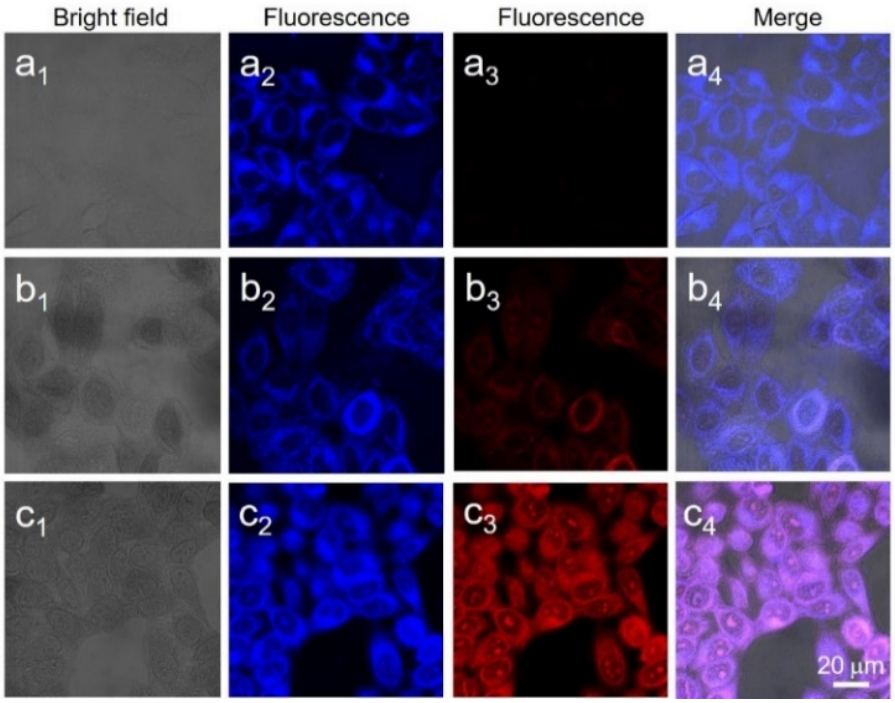

Figure 5. Confocal fluorescence microscopy images of HeLa cells incubated with 0 μM (a), 25 μM (b) and 50 μM (c) Fe^{3+} for 2 h, followed by further incubation with TPE-*o*-Py (10 μM) for 0.5 h. The fluorescence was recorded under 440-480 nm (a_2, b_2, c_2) and 620-700 nm (a_3, b_3, c_3) emission wavelength (the scale bar is equal to 20 μm).

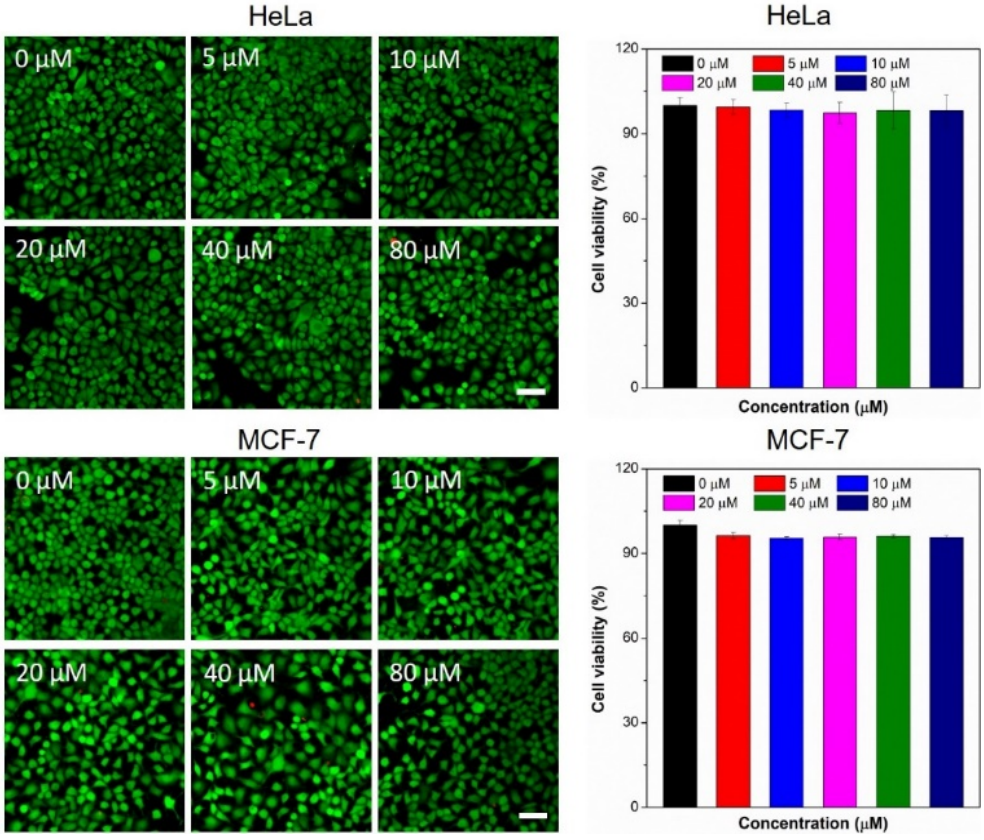

Figure 6 Fluorescence images of calcein AM/PI stained HeLa cells and MCF-7 cells (left panel) and CCK8 assay (right panel) of HeLa cells and MCF-7 cells treated by different

concentrations of TPE-*o*-Py. The scale bars equal to 100 μm, and the fields of vision (left panel) were randomly selected.

Table 1 The Ksp and pKa of differenct metal ions.[18]

Metal ions	Ksp	pKa	Metal ions	Ksp	pKa
$Fe(OH)_3$	4×10^{-38}	2.56	$Zn(OH)_2$	1.2×10^{-17}	9.55
$Al(OH)_3$	1.3×10^{-33}	4.07	$Cu(OH)_2$	2.2×10^{-20}	8.64
$Cr(OH)_3$	6.3×10^{-31}	4.96	$Pb(OH)_2$	1.2×10^{-15}	10.22
$Fe(OH)_2$	8.0×10^{-16}	10.16	$Mg(OH)_2$	1.8×10^{-11}	11.61
$Co(OH)_2$	1.6×10^{-15}	10.26	$Ca(OH)_2$	5.5×10^{-6}	13.44
[TPE-*o*-Py] = 1×10^{-5} M					

The table of contents entry: The article presents an aggregation induced emission (AIE) featured iron (III) probe from ortho-substituted pyridinyl-functionalized tetraphenylethylene (TPE-o-Py) by taking advantage of the position-dependent substituent effects. It displayed high sensitivity and selectivity toward iron (III) detection. The molecular recognition mechanism arises from the position isomer of ortho-substitution of TPE-*o*-Py which has a low acid dissociation constant (pKa) that is close to that of hydrolyzed Fe^{3+}. Importantly, TPE-*o*-Py as a light-up fluorescence probe could be employed for iron (III) sensing in living cells with a pronounced red-shift in fluorescence color.

Keyword: aggregation-induced emission, molecular recognition, iron (III), acid dissociation constant, cell imaging

Xing Feng, Ying Li, Xuewen He, Haixiang Liu, Zheng Zhao, Ryan T. K. Kwok, Mark R. J. Elsegood, Jacky W. Y. Lam, Ben Zhong Tang*

A Substitution-dependant Light-up fluorescence probe for selectively detecting Fe^{3+} ions and its cell imaging application